Available online at www.sciencedirect.com
ScienceDirect
Ceramics International 37 (2011) 3489–3497
CERAMICS INTERNATIONAL
www.elsevier.com/locate/ceramint

Polymer assisted isolation of hydroxyapatite from *Thunnus obesus* bone

Ramjee Pallela [a], Jayachandran Venkatesan [b], Se Kwon Kim [a,b,*]

[a] *Marine Bioprocess Research Center, Pukyong National University, Busan 608-737, Republic of Korea*
[b] *Department of Chemistry, Pukyong National University, Busan 608-737, Republic of Korea*

Received 21 March 2011; received in revised form 1 June 2011; accepted 6 June 2011
Available online 12 June 2011

Abstract

The combination of micro and nanostructured hydroxyapatite (HAp) was isolated from *Thunnus obesus* bone via thermal calcination method in the presence of polymers such as poly ethylene glycol (PEG), poly (ethylene glycol)-block-poly (propylene glycol)-block-poly (ethylene glycol) (PEG–PPG–PEG) and poly vinyl alcohol (PVA). The thermal stability, crystalline phase, chemical composition and morphology of the derived HAp were characterized by thermal gravimetric analysis, X-ray diffraction analysis, Fourier transform infrared spectroscopy and field emission scanning electron microscopy analysis. The physicochemical characteristic examination revealed that derived HAp was coherent with standard HAp data. Moreover, FE-SEM depicted significant difference in the crystal size of HAp derived with thermal calcination, with and without added polymers. The crystallinity of HAp isolated in the presence of polymer was lower than that obtained in the absence of polymers. The biocompatibility of the derived HAp crystals was checked with MC3T3-E1 osteoblastic cells by MTT assay and Hoechst-33342 staining. The biocompatibility of HAp derived by polymer assisted thermal calcination method revealed that it is less toxic as compared to HAp derived in the absence of polymer. As an inference, polymer assisted thermal calcination derived HAp is good in terms of the presence of combined micro and nanostructured HAp and its low toxicity will bring about new orthopaedic applications.

Keywords: Natural hydroxyapatite; Polymer assisted; *Thunnus obesus* bone

1. Introduction

In the recent past, considerable attention has been given to hydroxyapatite (HAp) for various biomedical applications due to its bioactivity and osteoconductive properties [1]. The advantage of HAp is its similarity to the inorganic portion of bone and teeth. Thus the usage of HAp in the bone graft substitute is ever increasing. In particular, the nanosize HAp has been widely used for various fields such as orthopedics, drug release and biomolecule separation [2]. For this, much attention has been paid by researchers to prepare nanosize HAp by chemical methods such as hydrothermal [3], liquid membrane [4], precipitation [5], radio frequency thermal plasma [6], ultrasonic precipitation [7], reverse micro emulsion [8], sol–gel [9] and polymer assisted method [10]. Among these, polymer assisted preparations are interesting to get nanostructured HAp crystals then compared to any other method. Thus we followed the same method to isolate HAp particle from the marine biowaste (Tuna bone).

Several polymer assisted methods have been developed to prepare HAp by many researchers [10]. A biomimetic method has been used to prepare spherical nano-HAp by using $Ca(NO_3)_2{\cdot}4H_2O$ and $(NH_4)_3PO_4{\cdot}3H_2O$ as reagents in the presence of poly ethylene glycol (PEG). It was observed that the crystallinity of HAp synthesized in the presence of PEG was higher than that synthesized in the absence of PEG [11]. Another research group used an organic template to prepare HAp via biomimetic mineralization method with poly vinyl alcohol (PVA) and sodium dodecyl sulfate (SDS) as the surfactant [12]. Apart from this, rod-like HAp has been synthesized by precipitating $Ca(NO_3)_2{\cdot}4H_2O$ and $(NH_4)_3PO_4{\cdot}3H_2O$ in the presence of polyacrylic acid followed by hydrothermal treatment [13]. The molecular weight of the polymer also plays a major role to prevent crystallization during the preparation of HAp. It has been reported that the development (size and shape) of the HAp nanocrystals precipitated in an aqueous solution of PVA get influenced by

* Corresponding author: Department of Chemistry, Pukyong National University, Busan 608-737, Republic of Korea. Tel.: +82 51 629 7094; fax: +82 51 629 7099.
E-mail address: sknkim@pknu.ac.kr (S.K. Kim).

0272-8842/$36.00
doi:10.1016/j.ceramint.2011.06.004

the molecular weight of the polymer and the crystal size of HAp decreased with increasing molecular weight of PVA [14]. Under the light of aforementioned studies, it can be inferred that these polymers participate in some chemical interaction while preparation of HAp by chemical method. In this course of study, HAp isolation has been tried from the natural biowaste of Tuna bone with polymer assisted thermal calcination method.

The waste of Tuna bone has recently become a serious threat for environment in Korea. Thus, these processed wastes of Tuna bone increases selectivity to isolate HAp and also decreases the environmental pollution. Moreover, HAp ceramics have been isolated from natural sources like cuttle fish bone [15], bovine bone [16–20] and fish bone [2,21–25]. But the isolation of HAp from natural source such as fish bone with polymer assisted thermal calcination method has not been reported anywhere. So in this study, we attempted to know the interaction of different types of polymers such PEG, PEG–PPG–PEG and PVA in the isolation of HAp from natural *Thunnus obesus* bone.

2. Materials and methods

2.1. Materials

Tuna bone was washed with hot water for 2 days to remove the traces of meat and skin. The washed bones were mixed with 1.0% sodium hydroxide (NaOH) and acetone to remove protein, lipids, oils and other organic impurities (bone and sodium hydroxide solid/liquid ratio was 1:50). After thorough washing, the bones were ground in a mortar pestle and then dried at 60 °C for 24 h. PEG $(–CH_2CH_2O–)_n$, $n = 6000$, was purchased from Yakuri Pure Chemicals Co., Ltd. Osaka, Japan. PVA $(–CH_2CHOH–)_n$, $n = 1500$ was obtained from Junsei Chemicals Co., Ltd. and PEG–PPG–PEG $(C_3H_6O{\cdot}C_2H_4O)_n$, $n = 8400$ was obtained from Sigma–Aldrich, USA.

2.2. Thermal calcination method

In thermal calcination method, 2 g of Tuna bone was placed in a silica crucible and subjected to a temperature of 900 °C in an electrical muffle furnace (Dongwan Scientific Co. A/S. 051, 245–7521) for 5 h.

2.3. Polymer assisted isolation of HAp

2 g of ground fish bone add 1% NaOH solution to remove soluble impurities, stirred for 12 h, and dried at 100 °C. The dried bone was mixed with 50% wt. amount of respective polymers and heated for 30 min at 250 °C. The polymer and bone mixture were transferred into silica crucible and calcined at 900 °C for 5 h.

2.4. Characterization

Thermal gravimetric analysis was achieved by the use of Pyris 7 TGA analyzers, Perkin Elmer Inc., USA with scan range from 50 to 900 °C at constant heating rate of 10 °C min^{-1} with continuous nitrogen flow. The stretching frequencies of samples were examined by Fourier transform infrared spectroscopy, Perkin Elmer (USA) and spectrum GX spectrometer within the range of 400–4000 cm^{-1}. The phase and crystallinity were evaluated using X-ray diffractometer (PHILIPS X'Pert-MPD diffractometer, Netherlands) and Cu Kα radiation 1.5405 Å over a range of 5–80° angle, step size 0.02, scan speed 4°/min with 40 kV voltage and 30 mA current. The XRD resultant spectra were compared with literature profile made by Joint Committee on Powder Diffraction Standards (JCPDS 09-0342/1996) to identify the compound. Morphology and chemical composition of HAp crystals were obtained by field emission scanning electron microscopy (FE-SEM JSM-6700F, Jeol, Japan).

2.5. In vitro cytotoxicity and cell proliferation assay

MC3T3-E1 (Osteoblast cell line) were cultured in α-MEM medium supplemented with 10% fetal bovine serum (FBS), 2 mM glutamine and 100 μg ml^{-1} penicillin–streptomycin and incubated at 37 °C in a humidified atmosphere with 5% CO_2. The biocompatibility of derived HAp has been analyzed with MC3T3-E1 and determined by measuring MTT dye absorbance in living cells. The cells were grown at a concentration of 2×10^3 cells/well in 96 well plates. After 24 h, cells were washed with fresh medium and were treated with different concentrations of HAp (31.25, 62.5, 125, 250, 500 and 1000 μg ml^{-1}). The cells without the addition of HAp crystals were taken as blank. After 1 day of incubation, the media was removed and 100 μl of MTT (5 mg ml^{-1}) was added and the cells were further incubated for 4 h. Finally 100 μl of DMSO was added to solubilize the formazan salt formed and the amount of formazan salt was determined by measuring the OD at 540 nm using a GENios® microplate reader (Tecan Austria GmbH, Austria). The relative cell viability was determined by the amount of MTT converted into formazan salt. Cell viability and cell proliferation of cells were quantified as a percentage compared to that of blank.

2.6. Morphological studies with optical microscopy and Hoechst staining 33342

The grown MC3T3-E1 cells were treated with different concentrations of HAp as mentioned for MTT assay, after 5 days, cells were washed twice and fixed in 2.5% glutaraldehyde in 1× PBS (phosphate buffered saline) for 1 day at −4 °C. The fixed cells were washed with PBS and their morphological changes were detected by a light microscope (CTR 6000; Leica, Wetzlar, Germany). After light microscopic examination, cells were stained with 10 μg ml^{-1} of the fluorescent DNA-binding dye, Bisbenzimide Hoechst 33342 (Sigma–Aldrich Corp., St. Louis, MO, USA) and incubated for 1 h at room temperature to reveal nuclear condensation/aggregation. The Hoechst-stained cells were visualized and photographed under fluorescence microscope (CTR 6000; Leica, Wetzlar, Germany).

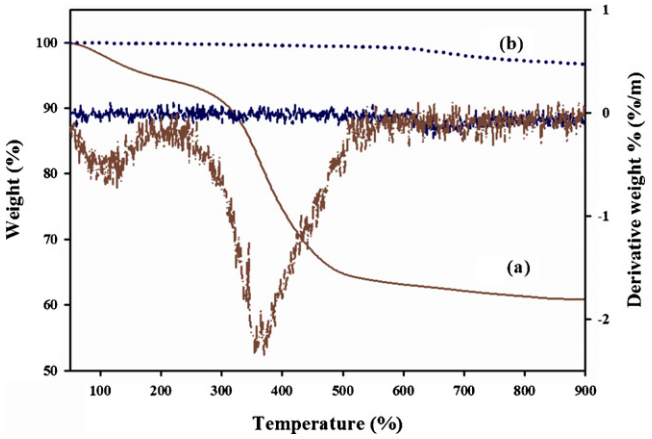

Fig. 1. Thermal gravimetric analysis of (a) raw bone and (b) polymer assisted derived HAp and its first derivative.

2.7. Statistics

Statistical analysis was performed by Sigma plot 10.0. All experiments were run in three replicates and the data were presented as the mean value ± standard deviation (SD) of each group.

3. Results and discussion

3.1. General observation

The raw bone was light yellow in color which revealed the presence of organic moieties with HAp. When raw bone was subjected to the polymer assisted thermal calcination method, the yellow color almost disappeared which indicated proper removal of organic moieties. Owing to its high thermal stability, HAp may not be removed by polymer assisted thermal calcination method. The color of the bone changed from yellow to white with thermal calcination at 900 °C, whereas proper

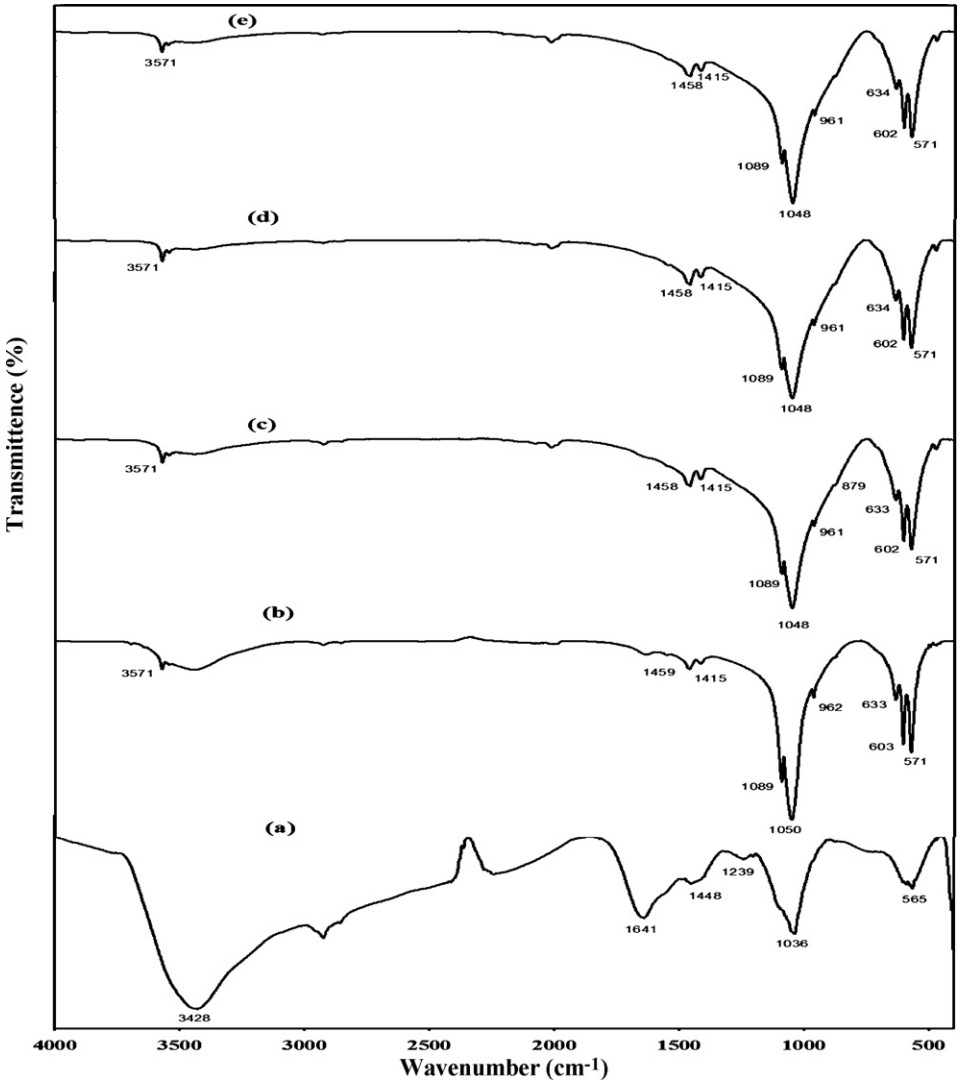

Fig. 2. Infrared spectrums of (a) raw bone, (b) thermal calcination method at 900 °C, (c) thermal calcination method at 900 °C with polyethylene glycol and (d) thermal calcination method at 900 °C with PEG–PPG–PEG (e) thermal calcination method at 900 °C with poly vinyl alcohol.

removal of organic materials was observed when the bone treated with PEG and PEG–PPG–PEG were thermally calcined. Finally the color of the derived HAp by polymer assisted thermal calcination method was pure white.

3.2. Thermo gravimetric analysis of derived HAp

TGA and DTG curves of raw Tuna bone and HAp produced by polymer assisted thermal calcination method are shown in Fig. 1. In TGA and DTG analysis, inflection was identified in raw bone at 100.4 and 365.6 °C. Sample weight (4.76 and 30.02%) was significantly reduced based on removal of water and organic moieties.

The first derivative curve of raw bone has shown a strong inflection at 365.6 °C due to the collagen and other organic moieties. In contrast, the first derivative curve of the apatite obtained by polymer assisted thermal calcination method had no significant peak at 365.6 °C. This confirmed the absence of collagen and organic moieties and used polymers in the derived product. With the aid of the above result, it is verified that HAp produced using polymer assisted thermal calcination method lack collagen and organic moieties. Thus the product obtained was optimum in quality as it was obtained in highly pure form.

3.3. Stretching frequency of derived HAp

Fig. 2 depicts FT-IR spectrum of raw bone and HAp extracted by thermal calcination and polymer assisted thermal calcination methods. As evident by the results, there was a clear difference in the spectral stretching between raw bone and derived HAp using proposed methods.

The presence of phosphate, carbonate and hydroxyl groups has been confirmed by FT-IR spectroscopy. A large number of bands appeared in spectra (1455, 1417, 1099, 1044, 963, 875, 632, 603 and 566 cm^{-1}) that were similar to HAp reference spectrum close to reported data [16,17]. Moreover, Fig. 2 also explains –OH bending vibration at 632 cm^{-1} and phosphate group at 500–1100 cm^{-1} which is in correlation with pure HAp

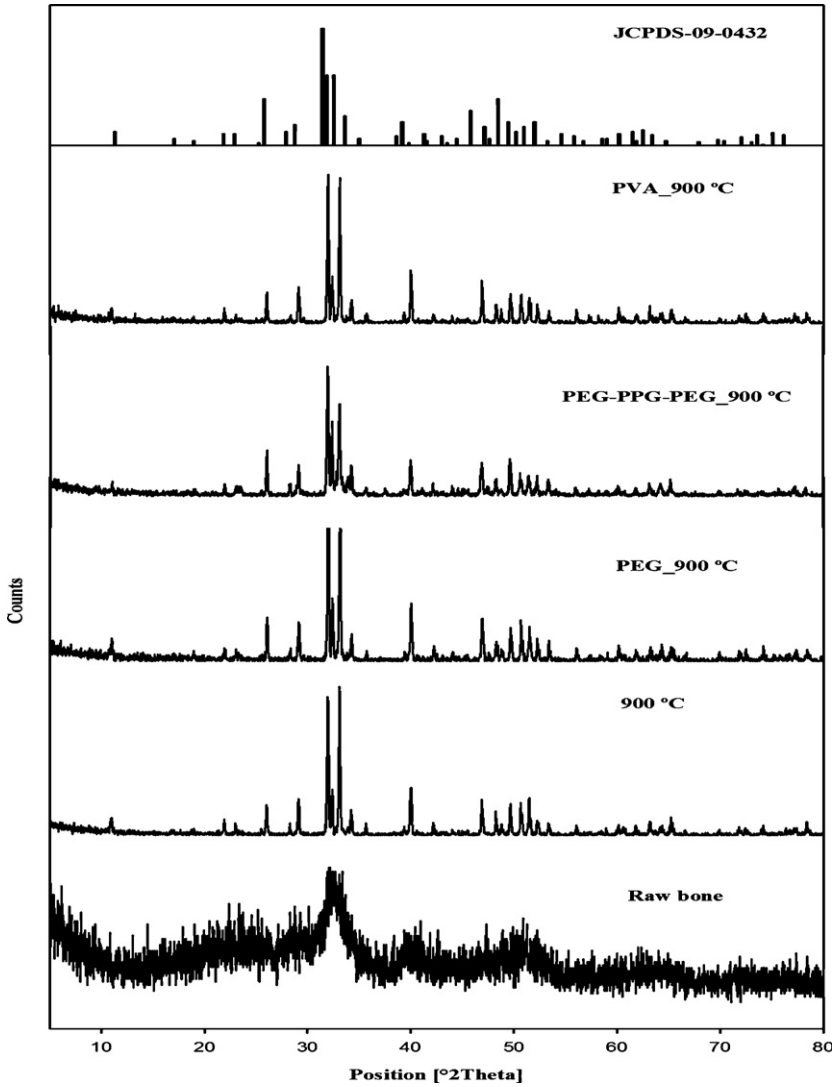

Fig. 3. X-ray diffraction spectrum of raw bone, thermal calcination method at 900 °C, polymer assisted derived HAp with PEG, PEG–PPG–PEG, PVA and reference HAp JCPDS-09-0432.

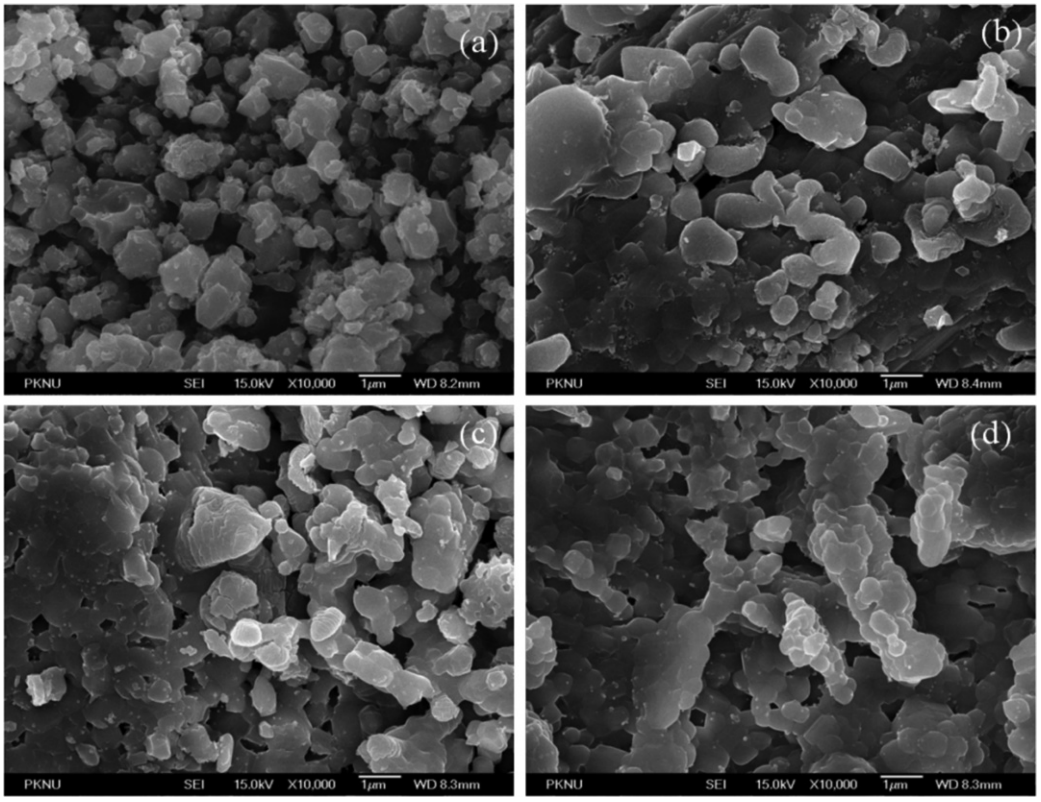

Fig. 4. Field emission-scanning electron microscopy images of (a) thermal calcination method at 900 °C polymer assisted derived HAp, (b) PEG, (c) PEG–PPG–PEG and (d) PVA.

Table 1
Important FT-IR stretching frequencies of HAp derived with thermal calcination and polymer assisted thermal calcination methods.

Methods	IR absorption bands (cm^{-1})	Description
Thermal calcination	1050, 1089	$\nu_3(PO_4^{3-})$
	962	$\nu_1(PO_4^{3-})$
	571	$\nu_4(PO_4^{3-})$
	1415, 1459	$\nu_3(CO_3^{2-})$
	634	Bending OH^-
	3571	ν(OH)
PEG with thermal calcination	1048, 1089	$\nu_3(PO_4^{3-})$
	962	$\nu_1(PO_4^{3-})$
	571	$\nu_4(PO_4^{3-})$
	1415, 1458	$\nu_3(CO_3^{2-})$
	633	Bending OH^-
	3571	ν(OH)
PEG–PPG–PEG with thermal calcination	1048, 1089	$\nu_3(PO_4^{3-})$
	961	$\nu_1(PO_4^{3-})$
	571	$\nu_4(PO_4^{3-})$
	1415, 1458	$\nu_3(CO_3^{2-})$
	634	Bending OH^-
	3571	ν(OH)
PVA with thermal calcination	1048, 1089	$\nu_3(PO_4^{3-})$
	961	$\nu_1(PO_4^{3-})$
	571	$\nu_4(PO_4^{3-})$
	1415, 1458	$\nu_3(CO_3^{2-})$
	634	Bending OH^-
	3571	ν(OH)

derived by thermal calcination and polymer assisted thermal calcination methods (Table 1).

Additionally, raw bone was found to have other absorption peaks at 2384 and 1544 cm^{-1} which correspond to N–H stretching and amide bonds, respectively; that are not found in the bone treated by the polymer [17]. In addition, sharp bands were observed at 632, 603 and 566 cm^{-1} that indicate the crystallinity of HAp [26]. The carbonated HAp has been proved to possess good biocompatibility, osteo integration, high

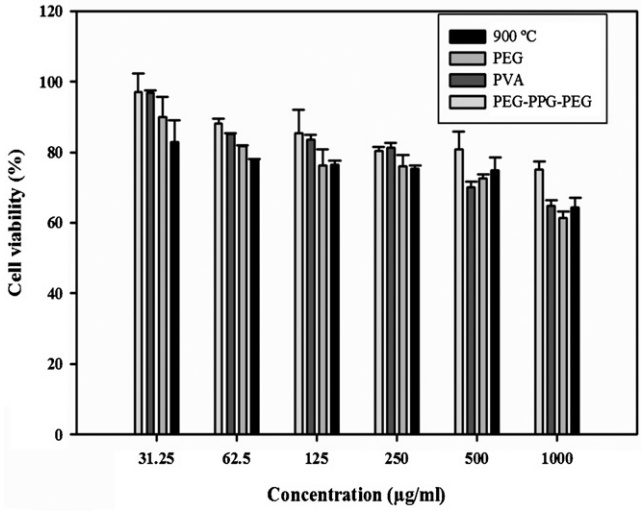

Fig. 5. Cytotoxity of MC3T3-E1 on thermal calcined and polymer HAp crystals at different concentration.

osteoconductivity and earlier bio resorption as compared to normal HAp [27].

3.4. X-ray diffraction analysis

The XRD reflection of derived HAp samples in the presence of different polymers is shown in Fig. 3. The results show that the diffraction peak of the raw bone is broad and wider as compared to the sharp peaks obtained by treatment with thermal calcination. Moreover, in the presence of polymers (PEG, PEG–PPG–PEG and PVA), no significant difference has been observed in the presence of polymers assisted HAp derivation.

3.5. Scanning electron microscopic analysis

The morphologies of derived HAp are shown in Fig. 4. Fig. 4(a) depicts the HAp derived with thermal calcination method, whereas Fig. 4(b)–(d) presents HAp derived by

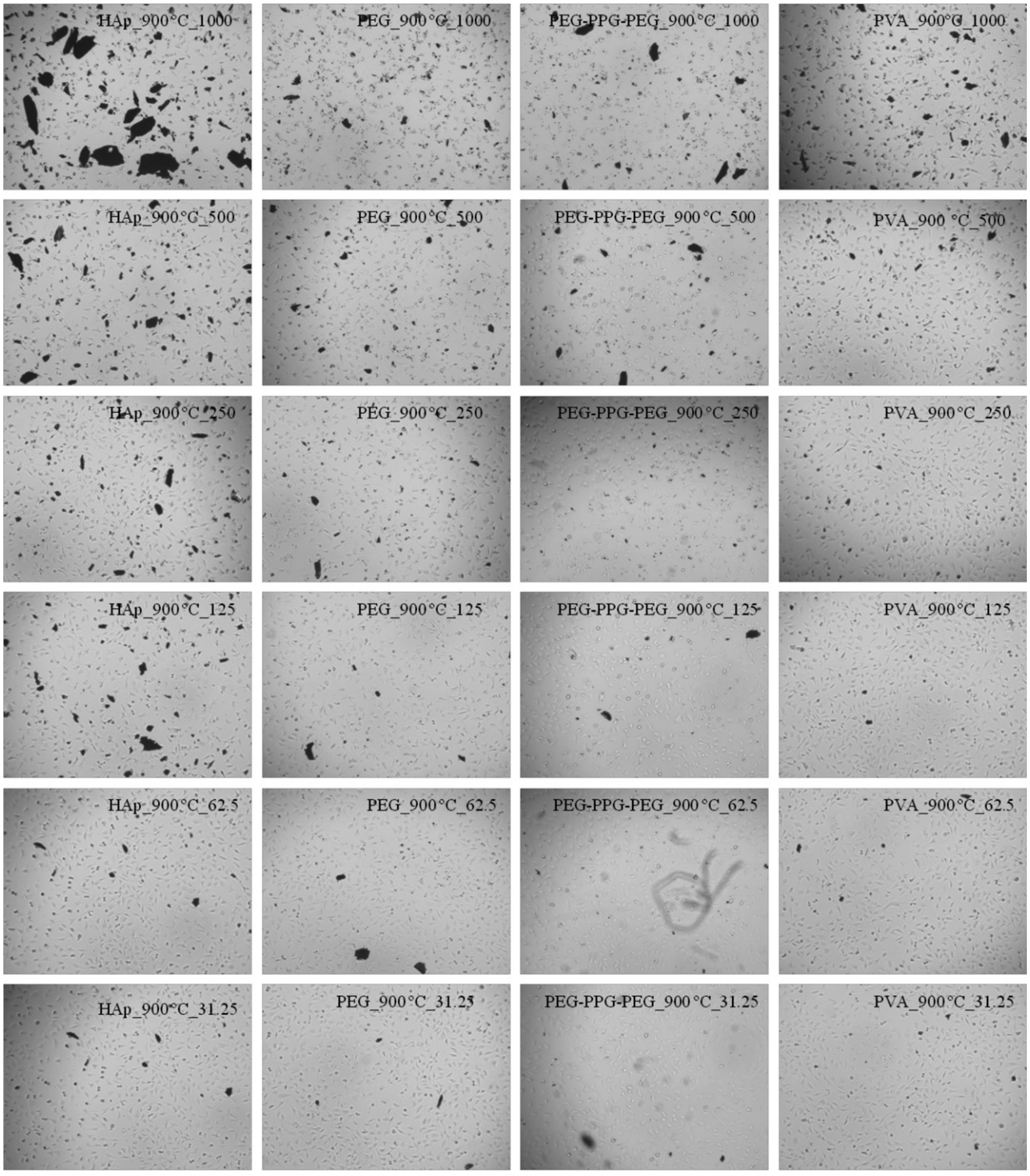

Fig. 6. Optical microscopy picture of MC3T3-E1 cells with thermal calcination and polymer assisted thermal calcination derived HAp.

polymer (PEG, PEG–PPG–PEG and PVA) assisted thermal calcination, respectively. The morphology of thermally derived HAp was well crystalline and crystals were dispersed. The HAp derived by polymer assistance was also well crystallized; however, significant difference has been observed in the crystals sizes of HAp obtained with thermal calcination and polymer assisted thermal calcination method. Polymer assisted derived HAp appears as a combination of nano and microstructure arrangement. In the entire examination, no fibrils like that of collagen and other organic moieties were observed in any of the methods employed for HAp derivation. Although not much difference was observed in the sizes of HAp crystals obtained by thermal calcination and polymer assisted thermal calcination method, the crystals were agglomerated when treated with thermal calcination method alone (300–1000 nm), whereas HAp crystal agglomeration was inhibited by polymer assisted thermal calcination method (PEG-230–1400 nm, PVA-200–800 nm and PEG–PPG–PEG-95–950 nm).

3.6. Cytotoxicity of derived HAp

There are several studies which suggest that HAp crystals are suitable for bone replacement and thus the usage of HAp in bone replacement is prevalent in biomedical field. In our study, cytotoxity of thermal derived HAp and HAp derived by polymer assisted thermal calcination was checked at different concentrations on MC3T3-E1 human osteoblast cells as shown in Fig. 5. The cytotoxicity of HAp crystals was observed at different days with different concentrations, the results revealed that thermally derived HAp showed cytotoxic effect on the proliferation of MC3T3-E1 cells at higher concentrations. On the contrary, HAp derived by polymer assisted thermal

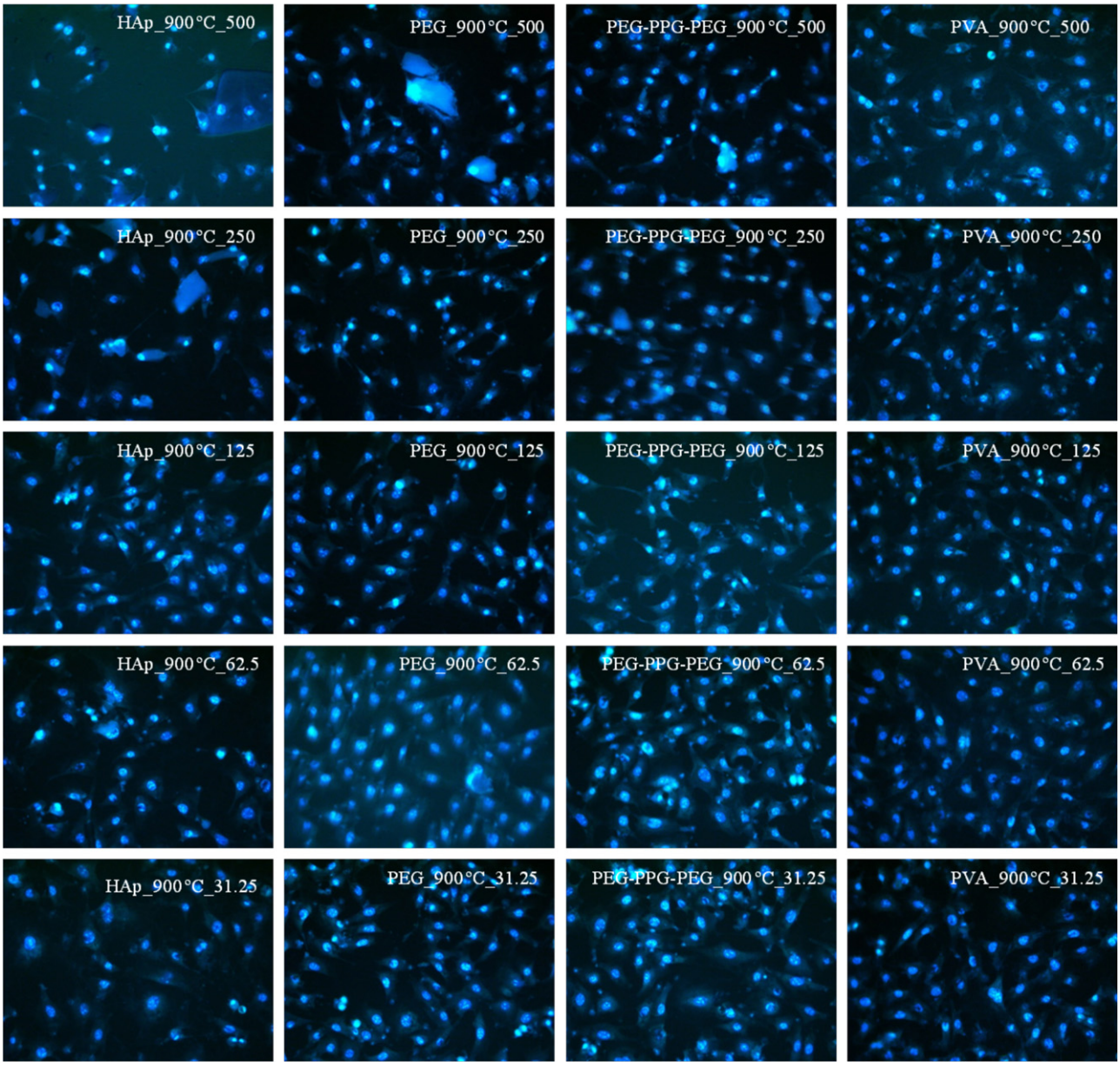

Fig. 7. Fluorescence Hoechst stained micrographs of MC3T3-E1 cells with thermal calcination and polymer assisted thermal calcination derived HAp.

calcination method was comparatively less cytotoxic. The molecular weight of polymer also played a major role in cytotoxic effect. From our results, we inferred that the cytotoxity of PEG–PPG–PEG derived HAp crystals was lesser when compared to that derived with PEG and PVA.

3.7. Morphological studies with optical microscopy and Hoechst stain 33342

The optical microscopy and fluorescence microscopic (Hoechst 33342 stain) images of MC3T3-E1 cells treated with HAp crystals are shown in Figs. 6 and 7, respectively. From the optical microscopy and after Hoechst staining, it was clear that cell count decreased with increasing concentrations of HAp derived by both the methods. The optical micrographs showed that the surfaces of the control culture plate were fully covered by MC3T3-E1 cells. Moreover, no cytotoxity was observed when treated with low concentrations of HAp (31.25, 62.5 and 125 $\mu g\ ml^{-1}$). Cytotoxicity has been observed at high concentrations of HAp particles (250, 500 and 1000 $\mu g\ ml^{-1}$) 1) compared with the control group. The average cell growth rate reduced by 40% on treatment with thermally calcined HAp. Further, few apoptotic cells were observed at high concentrations. However, significant difference has been observed between HAp derived through thermal calcination and polymer assisted thermal calcination methods. Cells grown with HAp derived by polymer assisted thermal calcination method have higher cell density as compared to thermally derived HAp treated cell line.

4. Conclusion

The combination of micro and nanostructured HAp was isolated successfully from *T. obesus* bone by polymer assisted thermal calcination method in the presence of different polymers such as PEG, PEG–PPG–PEG and PVA. The results indicated that the molecular weight of polymer used significantly affected the crystals size (PEG-230–1400 nm, PVA-200–800 nm and PEG–PPG–PEG-95–950 nm). Moreover, high purity of HAp was obtained using polymer assisted thermal calcination method. It was also observed that the cytotoxicity is limited when treated with HAp derived by polymer assisted thermal calcination method. From all the results, we concluded that polymer assisted thermal calcination method for isolation of HAp proposes great impact on industrial level production of HAp in future.

Acknowledgement

This work was supported by a grant from Marine Bioprocess Research Centre of the Marine Bio 21 Center funded by the Ministry of Land, Transport and Maritime, Republic of Korea.

References

[1] P.V. Giannoudis, H. Dinopoulos, E. Tsiridis, Bone substitutes: an update, Injury 36 (3 Suppl. 1) (2005) S20–S27.

[2] J. Venkatesan, S.K. Kim, Effect of temperature on isolation and characterization of hydroxyapatite from tuna (*Thunnus obesus*) bone, Materials 3 (10) (2010) 4761–4772.

[3] H. Zhang, K. Zhou, Z. Li, S. Huang, Plate-like hydroxyapatite nanoparticles synthesized by the hydrothermal method, Journal of Physics and Chemistry of Solids 70 (1) (2009) 243–248.

[4] S. Jarudilokkul, W. Tanthapanichakoon, V. Boonamnuayvittaya, Synthesis of hydroxyapatite nanoparticles using an emulsion liquid membrane system, Colloids and Surfaces A: Physicochemical and Engineering Aspects 296 (1–3) (2007) 149–153.

[5] S. Sarig, F. Kahana, Rapid formation of nanocrystalline apatite, Journal of Crystal Growth 237–239 (Part 1) (2002) 55–59.

[6] J.L. Xu, K.A. Khor, Z.L. Dong, Y.W. Gu, R. Kumar, P. Cheang, Preparation and characterization of nano-sized hydroxyapatite powders produced in a radio frequency (RF) thermal plasma, Materials Science and Engineering A 374 (1–2) (2004) 101–108.

[7] L.Y. Cao, C.B. Zhang, J.F. Huang, Synthesis of hydroxyapatite nanoparticles in ultrasonic precipitation, Ceramics International 31 (8) (2005) 1041–1044.

[8] G. Guo, Y. Sun, Z. Wang, H. Guo, Preparation of hydroxyapatite nanoparticles by reverse microemulsion, Ceramics International 31 (6) (2005) 869–872.

[9] W. Feng, L. Mu-sen, L. Yu-peng, Q. Yong-xin, A simple sol–gel technique for preparing hydroxyapatite nanopowders, Materials Letters 59 (8–9) (2005) 916–919.

[10] Y.-H. Tseng, C.-S. Kuo, Y.-Y. Li, C.-P. Huang, Polymer-assisted synthesis of hydroxyapatite nanoparticle, Materials Science and Engineering: C 29 (3) (2009) 819–822.

[11] C. Qiu, X. Xiao, R. Liu, Biomimetic synthesis of spherical nano-hydroxyapatite in the presence of polyethylene glycol, Ceramics International 34 (7) (2008) 1747–1751.

[12] W. Pon-On, S. Meejoo, I.M. Tang, Formation of hydroxyapatite crystallites using organic template of polyvinyl alcohol (PVA) and sodium dodecyl sulfate (SDS), Materials Chemistry and Physics 112 (2) (2008) 453–460.

[13] S. Zhang, K.E. Gonsalves, Preparation and characterization of thermally stable nanohydroxyapatite, Journal of Materials Science: Materials in Medicine 8 (1) (1997) 25–28.

[14] S. Mollazadeh, J. Javadpour, A. Khavandi, In situ synthesis and characterization of nano-size hydroxyapatite in poly(vinyl alcohol) matrix, Ceramics International 33 (8) (2007) 1579–1583.

[15] H. Ivankovic, G. Gallego Ferrer, E. Tkalcec, S. Orlic, M. Ivankovic, Preparation of highly porous hydroxyapatite from cuttlefish bone, Journal of Materials Science: Materials in Medicine 20 (5) (2009) 1039–1046.

[16] S. Joschek, B. Nies, R. Krotz, A. Göpferich, Chemical and physicochemical characterization of porous hydroxyapatite ceramics made of natural bone, Biomaterials 21 (16) (2000) 1645–1658.

[17] C.Y. Ooi, M. Hamdi, S. Ramesh, Properties of hydroxyapatite produced by annealing of bovine bone, Ceramics International 33 (7) (2007) 1171–1177.

[18] K. Haberko, M. Bucko, J. Brzezinska-Miecznik, M. Haberko, W. Mozgawa, T. Panz, A. Pyda, J. Zarebski, Natural hydroxyapatite—its behaviour during heat treatment, Journal of the European Ceramic Society 26 (4–5) (2006) 537–542.

[19] X. Lü, Y. Fan, D. Gu, W. Cui, Preparation and characterization of natural hydroxyapatite from animal hard tissues, Key Engineering Materials 342 (2007) 213–216.

[20] K. Haberko, M. Buko, M. Haberko, W. Mozgawa, A. Pyda, J. Zarbski, Natural hydroxyapatite—preparation and properties, Engineering Biomaterials 6 (2003) 32–37.

[21] T. Coelho, E. Nogueira, W. Weinand, W. Lima, A. Steimacher, A. Medina, M. Baesso, A. Bento, Thermal properties of natural nanostructured hydroxyapatite extracted from fish bone waste, Journal of Applied Physics 101 (2007) 084701.

[22] M. Ozawa, K. Satake, R. Suzuki, Removal of aqueous chromium by fish bone waste originated hydroxyapatite, Journal of Materials Science Letters 22 (7) (2003) 513–514.

[23] M. Ozawa, S. Suzuki, Microstructural development of natural hydroxyapatite originated from fish-bone waste through heat treatment, Journal of the American Ceramic Society (USA) 85 (5) (2002) 1315–1317.
[24] K. Prabakaran, S. Rajeswari, Development of hydroxyapatite from natural fish bone through heat treatment, Trends in Biomaterials Artificial Organs 20 (2006) 20–23.
[25] J. Venkatesan, Z.-J. Qian, B. Ryu, V.T. Noel, S.-K. Kim, A comparative study of thermal calcination and an alkaline hydrolysis method in the isolation of hydroxyapatite from *Thunnus obesus* bone, Biomedical Materials 6 (3) (2011) 035003.
[26] M. Markovic, B. Fowler, M. Tung, Preparation and comprehensive characterization of a calcium hydroxyapatite reference material, Journal of Research of the National Institute of Standards and Technology 109 (6) (2004) 553–568.
[27] E. Landi, G. Celotti, G. Logroscino, A. Tampieri, Carbonated hydroxyapatite as bone substitute, Journal of the European Ceramic Society 23 (15) (2003) 2931–2937.